PHYSICAL REVIEW A **77**, 052704 (2008)

Feshbach-resonance-mediated annihilation in positron interactions with large molecules

J. A. Young* and C. M. Surko
Department of Physics, University of California, San Diego, 9500 Gilman Drive, La Jolla, California 92093-0319, USA

(Received 5 March 2008; published 5 May 2008)

Measurements of positron-on-molecule annihilation have established that positrons attach to a variety of molecules via vibrational Feshbach resonances (VFRs). These resonances, in turn, result in greatly enhanced positron annihilation rates beyond those expected in simple collisions. A recent paper [J. A. Young and C. M. Surko, Phys. Rev. Lett. **99**, 133201 (2007)] described experimental studies and analysis of positron annihilation in large molecules. Presented here is a more complete description of those results as well as data and analysis. Positron-molecule binding energy data are presented for twenty-five molecules, including the relatively deeply bound species 1-chlorohexane, benzene, and naphthelene. When a relatively weak dependence of resonant annihilation rate on incident positron energy and binding energy is removed, the resulting rates for hydrocarbons are shown to obey a universal scaling as a function of the number of vibrational degrees of freedom. Previously measured annihilation rates for alkanes using thermal positrons at 300 K are shown to be in quantitative agreement with measurements at higher energies. Results are presented for partially fluorinated hydrocarbons, providing evidence that the unusual suppression of resonant annihilation observed in these molecules occurs via a vibrational deexcitation process. The role of molecular temperature and inelastic escape channels in VFR-mediated positron annihilation in molecules is discussed. The implications of these results for theories of the annihilation process are also discussed.

DOI: 10.1103/PhysRevA.77.052704 PACS number(s): 34.80.Uv, 34.50.−s, 78.70.Bj, 71.60.+z

I. INTRODUCTION

Positrons are of interest in many fields of science and technology including astrophysics, materials science, and medicine, yet many elementary processes involving these antiparticles are still poorly understood [1,2]. One example is the low-energy interaction of positrons with ordinary molecules. It is now known that positrons with energies below the threshold for positronium formation can attach to many molecules including hydrocarbons. Furthermore, they exhibit greatly enhanced annihilation rates beyond those expected on the basis of simple collisions. This occurs via vibrational Feshbach resonances (VFRs), in which an incident positron excites a molecular vibration and becomes attached to the molecule [3–6]. This process enhances the interaction of the positron with the molecular electrons, thereby increasing greatly the probability of annihilation. The ultimate fate of the positron in such a resonant state is determined by the competition between positron-electron annihilation and reemission from the target by deexcitation of a vibrational mode in the molecule.

Annihilation rates are typically expressed in terms of Z_{eff}, which is the ratio of the annihilation rate λ for a given density of molecules n_m to the rate for the same density of free electrons. Specifically, $Z_{\text{eff}}=\lambda/(\pi r_0^2 c n_m)$, where c is the speed of light and r_0 is the classical electron radius. A simple scattering picture suggests that $Z_{\text{eff}} \lesssim Z$, the total electronic charge on the molecule [3,7–9]. However, for many molecules, $Z_{\text{eff}} \gg Z$ because of VFR-mediated capture. For small molecules such as methyl halides, there is now quantitative agreement between experiment and a theory that describes resonant annihilation in terms of VFR due to infrared-active modes [10]. As the size of a molecule increases, the positron-molecule interaction becomes more complicated and theoretical predictions become more difficult [11]. Discussed here is the case of large molecules (e.g., hydrocarbons with two or more carbon atoms) in which the physics of the annihilation process appears to involve other processes not presently understood.

Annihilation in alkanes (C_nH_{2n+2}) provides a good starting point for this discussion. Shown in Fig. 1 is annihilation rate $Z_{\text{eff}}(\epsilon)$ as a function of incident positron energy ϵ for the

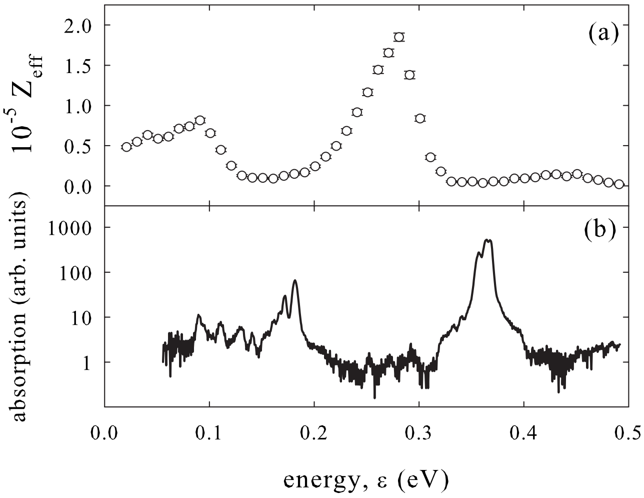

FIG. 1. (a) Z_{eff} spectrum [5]; and (b) infrared absorption spectrum (log scale, arbitrary units) [12] for hexane. Note that, when the 80 meV downshift of the Z_{eff} spectrum due to the positron-hexane binding energy is taken into account, the strong peaks in the two spectra occur at the same energy.

---

*Present address: Department of Chemistry, University of Nevada, Las Vegas, 4505 Maryland Pkwy., Las Vegas, Nevada 89154-4003.

1050-2947/2008/77(5)/052704(14)

six carbon alkane, hexane (C_6H_{14}) [5]. It is compared with the infrared absorption spectrum [12], which is a measure of the positron-hexane electric dipole coupling. As with other alkanes, hexane has large annihilation resonances associated with its fundamental vibrations, roughly paralleling resonances in the infrared spectrum. The dominant peak at $\epsilon \sim 285$ meV is due to excitation of the C-H stretch vibrational mode, and so it is referred to here as the "C-H stretch peak." It is downshifted below the mode energy of ~ 365 meV by 80 meV because of the positron-hexane binding. The shape of the peak is due entirely to the energy spread of the trap-based positron beam [10]. The enhancement of the spectrum at energies $\epsilon \leq 0.13$ eV is due to VFR from other vibrational modes (e.g., C-C modes and C-H bend modes).

One distinguishing feature of large molecules is their extraordinarily intense annihilation resonances. The height of the C-H stretch resonance at 285 meV in hexane is over two orders of magnitude larger than that in 1-bromomethane [6]. In fact, while the positron binding energy in alkanes increases linearly with molecular size (i.e., the number of carbons n), the magnitudes of the annihilation peaks rise exponentially with n. Since the number of fundamental vibrations increases only linearly with the molecular size, single-mode VFR cannot explain the magnitude of Z_{eff} in large molecules. Furthermore, the shapes of alkane Z_{eff} spectra change little with molecular size, indicating that if there are any additional resonances, they are degenerate with the single-mode VFR.

In this paper we present studies of VFR-mediated annihilation in large molecules. Data are presented for molecules such as 1-chlorohexane and the aromatic molecules, benzene and naphthalene, which have much larger binding energies than alkane molecules of comparable size. Data are also presented for second (i.e., "positronically excited") bound states that are observed in very large alkanes (i.e., $n \geq 12$). A key finding is that the dependence of the annihilation rate on incident positron energy and binding energy is given by simple theoretical considerations and is much weaker than that resulting from increases in the number of molecular vibrational degrees of freedom. We argue here that these results imply inelastic escape channels are mostly inoperative in large molecules. An analysis is presented showing that previously measured values of Z_{eff} in alkanes using a 300 K distribution of thermal positrons are in good agreement with the energy resolved measurements at higher energies.

One class of molecules with distinctly different behavior is alkanes with one or more hydrogens replaced by fluorines [5,6]. Presented here are data for partially fluorinated alkane molecules which provide evidence that an unusually effective inelastic escape channel is responsible for this difference. Also, a study of VFR-enhanced annihilation rates in alkanes as a function of the temperature of the molecules is briefly discussed [13]. This study indicates that molecular temperature has only a weak effect on the magnitude of Z_{eff}. For example, decreasing the molecular temperature of pentane by a factor of 2 from 300 to 150 K results in only a modest increase in the magnitudes of the annihilation rates, occurring mostly at lower energies. This result is interpreted as additional evidence that inelastic escape channels generally play a minor role in VFR-enhanced annihilation in hydrocarbons.

The implications of these results for theoretical models of positron binding and VFR-enhanced annihilation are discussed. Evidence presented here supports the theory [14] that additional, multimode vibrational excitations, accessed indirectly via intramolecular vibrational relaxation (IVR) following positron capture, can explain the observed enhancement in annihilation rates.

This paper is organized as follows. Key theoretical concepts and parameters are introduced. The experimental apparatus and procedures used in these studies are briefly described. Then data are presented for deeply bound species, including those with second positronic bound states. Accumulated data from a total of 27 species are used to deduce a universal scaling of the resonant annihilation rate as a function of molecular size. Measurements of Z_{eff} for thermal positrons at 300 K are shown to be consistent with energy resolved measurements made at higher positron energies. Results are presented for partially substituted alkanes and for alkanes as a function of molecular temperature. Additional phenomena such as multimode VFR and trends in binding energy are also described. Finally, the state of our understanding of the Feshbach-resonant annihilation process in large molecules is summarized and possible directions for future research are discussed.

II. THEORY OF RESONANT ANNIHILATION

There is now a successful, quantitative theory of Feshbach-resonant positron annihilation in small molecules in the case where all of vibrational modes have significant dipole coupling to the incident positron [11,15]. This theory predicts that the annihilation rate as a function of positron energy can be described as a sum of resonances whose magnitudes are given by an energy-dependent factor g which is described below. For large molecules, quantitative predictions are not yet possible, partly because their vibrational spectra are far more dense. However, one can still use the VFR formalism to describe Z_{eff} averaged over a small energy interval containing many resonances [3,14]. In atomic units,

$$Z_{\mathrm{eff}} = \frac{2\pi^2 \rho_{ep}}{k} \frac{\Gamma^e(\epsilon)}{\Gamma(\epsilon)} \rho(\epsilon + \epsilon_b), \tag{1}$$

where $k \propto \sqrt{\epsilon}$ is the positron momentum, ρ_{ep} is the electron-positron contact density in the bound state, Γ^e is the positron resonance elastic (i.e., capture) width, Γ is the total resonance width at positron energy ϵ, and $\rho(\epsilon + \epsilon_b)$ is the density of accessible vibrational states. Theory and experiment indicate that the positron-molecule binding energy ϵ_b is practically independent of the vibrational mode that is excited [3,5].

The resonant annihilation rate is proportional to the rate of capture Γ^e and the probability of annihilation following capture, which is proportional to ρ_{ep}/Γ. The total width $\Gamma = \Gamma^a + \Gamma^e + \Gamma^i$ includes all competing post-capture processes, including the rate of annihilation Γ^a, the rate of elastic reemission Γ^e, and the rate of inelastic reemission Γ^i. It is usually assumed that $\Gamma \approx \Gamma^e$ but until now, this has only been

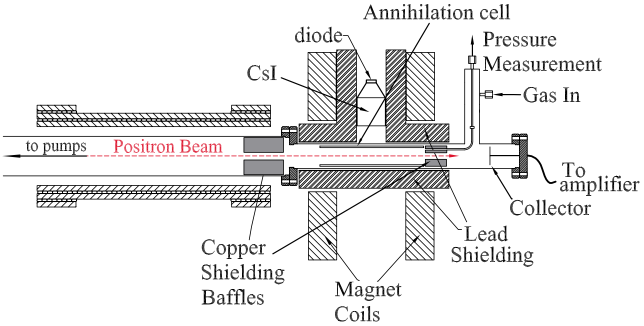

FIG. 2. (Color online) Schematic diagram of the experimental apparatus used for studies of test gases at 300 K. See text for details.

verified for small molecules. In some molecules, the contribution of Γ^i may be important and can result in a measurable reduction in the resonant Z_{eff} above the specific energy threshold associated with a given mode of inelastic escape.

For a simple s-wave model of the bound-state positron wave function, $\rho_{ep} \propto \sqrt{\epsilon_b}$ [16]. In this case, the explicit dependence of each Z_{eff} resonance on ϵ and ϵ_b in Eq. (1) is through a simple scale factor

$$g = \sqrt{\epsilon_b/\epsilon}, \tag{2}$$

where $\epsilon = \omega_\nu - \epsilon_b$ and ω_ν is the energy of the vibrational excitation involved. Beyond this factor, Z_{eff} involves the unique dynamics between the positron, nuclei, and electrons.

These dynamics play an increasingly important role in larger molecules such as hydrocarbons with two or more carbons. For these molecules, the resonant annihilation rates grow far too rapidly relative to the increase in the number of vibrational degrees of freedom to be fully explained by simple single-mode VFR. There is circumstantial evidence that the magnitude of the annihilation rate can be greatly enhanced by the large bath of multimode molecular vibrations that are not directly coupled to the incident positron [3,14]. This may occur through the process of IVR, in which energy from the initial vibrational excitation (e.g., that of a fundamental) rapidly relaxes into this bath of quasidegenerate vibrations, slowing down the process of positron detachment and hence increasing the annihilation probability. In this limit, one can consider $\rho(\epsilon + \epsilon_b)$ to be the density of these "dark" vibrational states instead of just the density of states that are directly coupled to the free positron (i.e., singly excited modes).

III. EXPERIMENTAL PROCEDURES

The experimental procedures used to measure molecular annihilation rates as a function of positron energy have been discussed in detail elsewhere [4–6]. The experimental apparatus is shown schematically in Fig. 2. Moderated positrons are accumulated and cooled in a three-stage buffer-gas trap using a gas mixture of N_2 and CF_4. Pulses of positrons are then magnetically guided through a cylindrical electrode of a cell filled with the test gas. Incident positron energies are adjusted by varying the electrical potential of this cell. Total positron energy is obtained from measurements using the gas cell as a retarding potential analyzer (RPA) and assuming a Maxwellian perpendicular energy distribution with a temperature of 25 meV [10]. To account for that perpendicular energy, a 12 meV correction is added to the RPA energy for all Z_{eff} spectra. Note that this is 4 meV less than the correction procedure used previously (e.g., in Refs. [5,6,17]). Further details of the beam energy distribution are described in Ref. [10]. Spectra of Z_{eff}, including that shown in Fig. 1, are plotted as a function of total positron energy ϵ.

Since the natural widths Γ of vibrational resonances are much smaller than the energy spread of the positron beam Δ, the observed widths and shapes of resonances, such as that at 285 meV in hexane, are explained entirely by the beam energy distribution. Furthermore, the observed magnitudes are reduced by a factor of Δ/Γ relative to the natural magnitudes.

Different systems are used to deliver gas and vapor to the annihilation cell. For species that are gases at 300 K, the flow into the annihilation cell is controlled by a piezoelectric valve. The voltage on this piezovalve is regulated via a proportional-integral-derivative (PID) controller using the pressure read with a capacitance manometer. This results in a reliable and steady gas cell pressure during the course of the experiment, limited only by the accuracy of the manometer and the response of the piezovalve. Typically the pressure can be set with micro-Torr precision. The liquid delivery system, while offering less control, permits studies of a broad range of target species. Liquid samples are deposited in a test tube, and a freeze-pump-thaw procedure is used to eliminate contaminants. The sample is then placed in a temperature-regulated bath in order to produce a constant vapor pressure, and a needle valve is used to leak vapor into the annihilation cell. In this case, there is no feedback control of the pressure. In spite of this, the pressure is relatively stable, as determined by ion gauge measurements before and after a data run. This system can also be used with gasses that have high boiling points (i.e., close to room temperature) and pulverized solid samples, such as naphthalene, provided they have an appreciable vapor pressure at room temperature [18].

Some vapors must be run at pressures below the range of the capacitance manometer to avoid saturation of the γ-ray detector. In this case, the pressure of the test species is measured at a higher pressure by both the manometer and the ion gauge to determine the ion gauge calibration factor. A few species, such as naphthalene, have extremely low vapor pressures, which complicates this procedure [18]. Even with a coarser needle valve and mild heating, it was difficult to get accurate pressure calibrations for these molecules. For naphthalene, an ion gauge calibration factor of 6 was used as an estimate, based on the measured value of 6.3 for the thermal positron apparatus described in Ref. [19]. For alkanes with 14 and 16 carbons, no pressure estimates were possible.

Single quanta from two-γ annihilation events are detected using a CsI detector. Typically, the positron pulses are allowed to pass through the gas cell four or five times while annihilation events are recorded, with total scattering kept below 15%. Absolute values of Z_{eff} are obtained from measurements of the pulse strength, the path length and the test-

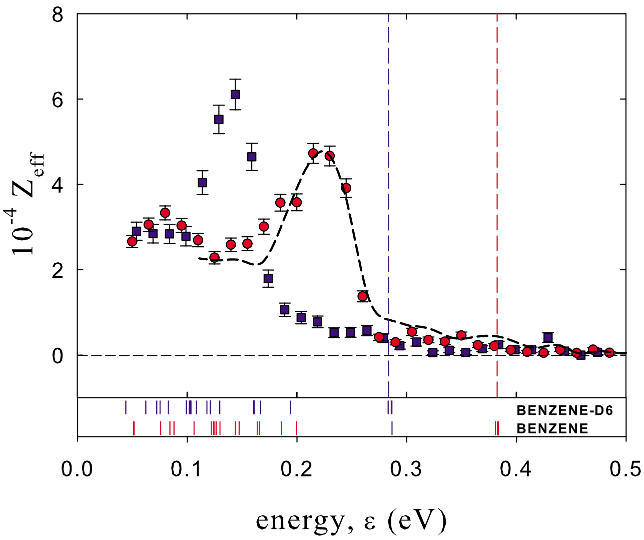

FIG. 3. (Color online) $Z_{\rm eff}$ spectra for (red ●) benzene and (blue ■) benzene-d6 from Ref. [20]. The vertical dashed lines mark the average energies of the C-H stretch modes of benzene and the C-D stretch modes of benzene-d6. The dashed curve is the benzene-d6 spectrum with the derived mode energy $\epsilon_v = \epsilon - \epsilon_b$ scaled by 1.28, assuming $\epsilon_b = 150$ meV; and the height is scaled by 0.78. The lower panel indicates the positions of the vibrational modes in benzene and benzene-d6 from Ref. [12].

gas pressure. Uncertainties in these parameters are estimated to result in a 20% overall uncertainty in the absolute magnitude of $Z_{\rm eff}$. A separate, specially designed cell, described in Ref. [13], was used for studies of annihilation as a function of molecular temperature. It is capable of cooling target gases down to 100 K.

IV. RESULTS

A. Dependence of $Z_{\rm eff}$ on binding energy and molecular size

The $Z_{\rm eff}$ spectra have been measured for a number of hydrocarbon species in addition to the simple alkanes [4,5]. Many of these molecules have clearly identifiable annihilation resonances, the C-H stretch-mediated resonances typically being most prominent, from which we deduce values of positron binding energy. In order to better distinguish the role of binding energy from that of molecular size, we start by examining benzene and chlorohexane. These two molecules have unusually large binding energies for their size.

Shown in Fig. 3 is a recent measurement of the energy-resolved annihilation spectrum for benzene [20]. A broad background present in a previous measurement [6] was eliminated by lowering the transport energy to prevent positronium formation outside the gas cell. Both the previous spectrum and that in Fig. 3 exhibit a large peak at an incident positron energy $\epsilon \sim 230$ meV. The C-H stretch modes that usually produce the dominant resonances in hydrocarbons occur as a collection of modes centered near 380 meV in benzene [12]. Assuming that this feature in benzene is the C-H stretch peak would imply a positron binding energy of 150 meV, much larger than that of a similarly-sized alkane molecule hexane shown in Fig. 1.

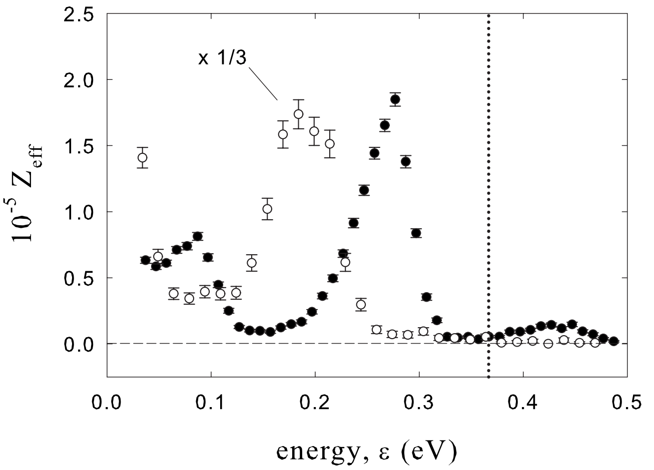

FIG. 4. $Z_{\rm eff}$ spectra for (○) 1-chlorohexane scaled by 1/3 [20], and (●) hexane [5]. Note the large increase in binding energy of the chlorinated compound.

To confirm the identity of this peak, the annihilation spectrum of fully deuterated benzene (benzene-d6) was also measured. Since deuterated and nondeuterated species have same electronic ground states, a common binding energy is assumed, consistent with previous observations for other hydrocarbons [4]. The $Z_{\rm eff}$ spectrum for benzene-d6, shown in Fig. 3, is dominated by a single peak at 148 meV with a plateau on the low-energy side. These data, taken together, show that the peaks in both benzene and benzene-d6 are due to the C-H stretch mode, indicating a common binding energy of 150 meV. In particular, upon correcting for this value of the binding energy, the ratio of the energies of the peaks is 1.28, which is very close to 1.34, the expected ratio of the C-H and C-D stretch mode energies. Also, similar to small molecules [15,20] and consistent with Eq. (1) above, the ratio of the peak heights is given by the ratio of the g factors for the two molecules, which is 0.78. Making these scaling adjustments to the spectrum of benzene-d6 results in a curve strikingly similar in magnitude and spectral shape to that of benzene. This is shown by the dashed curve in Fig. 3. The significance of this result will be discussed in more detail later.

Superficially, positron-benzene interactions appear to differ significantly from positron-alkane interactions. The binding energy of benzene ($\epsilon_b = 150$ meV) is as large as that of nonane (the nine carbon alkane), in spite of benzene having only six carbons such as hexane ($\epsilon_b = 80$ meV), and one more atom than propane ($\epsilon_b \sim 10$ meV). Benzene also has a relatively small $Z_{\rm eff}$ value which is between that of butane and pentane. As discussed in Sec. IV G, the unusually deep binding energy of benzene may be due to the unique electronic structure of this aromatic molecule.

Another molecule with deep binding is 1-chlorohexane. The $Z_{\rm eff}$ spectra for 1-chlorohexane and hexane from Ref. [20] are shown in Fig. 4. The former has binding energy of 175 meV and a C-H stretch mode peak height $Z_{\rm eff}^{\rm CH} = 5.2 \times 10^5$. Both of these parameters are substantially larger than those in hexane ($\epsilon_b = 80$ meV; $Z_{\rm eff}^{\rm CH} = 1.8 \times 10^5$), even though the number of atoms is the same, and the number of valence electrons is similar. The increased binding energy of

1-chlorohexane relative to that of hexane is discussed in Sec. IV G.

When 1-chlorohexane and hexane are normalized by g, the ratio of the C-H stretch peak heights, while not unity, is reduced from 2.8 to 1.6. This suggests their dependence on ϵ and ϵ_b is roughly similar to that of benzene. This contrasts sharply with 1-fluorohexane, which has a much smaller C-H stretch-peak height, even after normalization [5,6]. In Sec. IV C, it will be shown that 1-fluorohexane has an additional positron escape mechanism not present in 1-chlorohexane or hexane.

In addition to the molecules discussed above, binding energies and C-H stretch resonance magnitudes were measured for cyclopropane and cyclohexane [6], the 1-halomethanes (CH_3X, where X is F, Cl, and Br) [6], methanol (CH_3OH) [11], and the two-ring aromatic, naphthalene. We have also studied the first and second (i.e., positronically excited) bound state resonances in three large alkanes [20]. Figure 5(a) shows C-H stretch resonance Z_{eff} vs binding energy for a variety of species. While the alkanes fall on a single curve, other species such as benzene and 1-chlorohexane are scattered below this curve. This suggests that Z_{eff} is strongly influenced by factors other than the binding energy.

In small molecules, such as the 1-halomethanes, the factor $g=\sqrt{\epsilon_b/\epsilon}$ alone provides a complete description of the relative magnitudes of the Z_{eff} resonances, enabling absolute predictions of Z_{eff} spectra [10,11]. While such absolute predictions are not possible in larger molecules, Eq. (1) suggests that the dependence on ϵ and ϵ_b may be the same. This dependence is normalized out in Fig. 5(b), which shows Z_{eff}/g vs the number of atoms. This parametrization is a clear improvement over that of Fig. 5(a). For reference, data for a variety of species including most of those shown in Fig. 5(b) are also presented in Table I. [Not shown in either Fig. 5(b) or Table I is the second bound state of dodecane due to a large uncertainty in $1/g$ caused by the near-zero value of this molecule's binding energy.]

In general, Fig. 5(b) and Table I indicate that hydrocarbons with similar numbers of atoms have similar normalized C-H stretch peak heights. Unlike in Fig. 5(a), benzene is no longer an outlier. Other molecules such as cyclohexane and cyclopropane, which have relatively small Z_{eff} values [6], are also close to the trend line of the alkanes. The best empirical fit to this trend is a simple power law $Z_{\text{eff}}/g=2.3\times N^{\eta}$, where N is the number of atoms and $\eta=4.1$. The only major exceptions to this power-law scaling, of which we are aware, are the fluorine-substituted compounds such as 1-fluorohexane and 1-fluorononane [not shown in Fig. 5(b)] [5,6]. The unique nature of these molecules is discussed in Sec. IV C below.

Also not shown in Fig. 5(b) are data for tetradecane, the 14-carbon alkane, and hexadecane, the 16-carbon alkane. The absolute Z_{eff} values for these waxlike compounds are uncertain due to difficulties in determining the absolute test-gas pressure. As will be discussed later, these molecules exhibit resonances due to both first and second (i.e., positronically excited) bound states. The scaled values, Z_{eff}/g, from their first and second C-H stretch peaks, shown in Table I, are nearly identical, providing further support for this normalized representation.

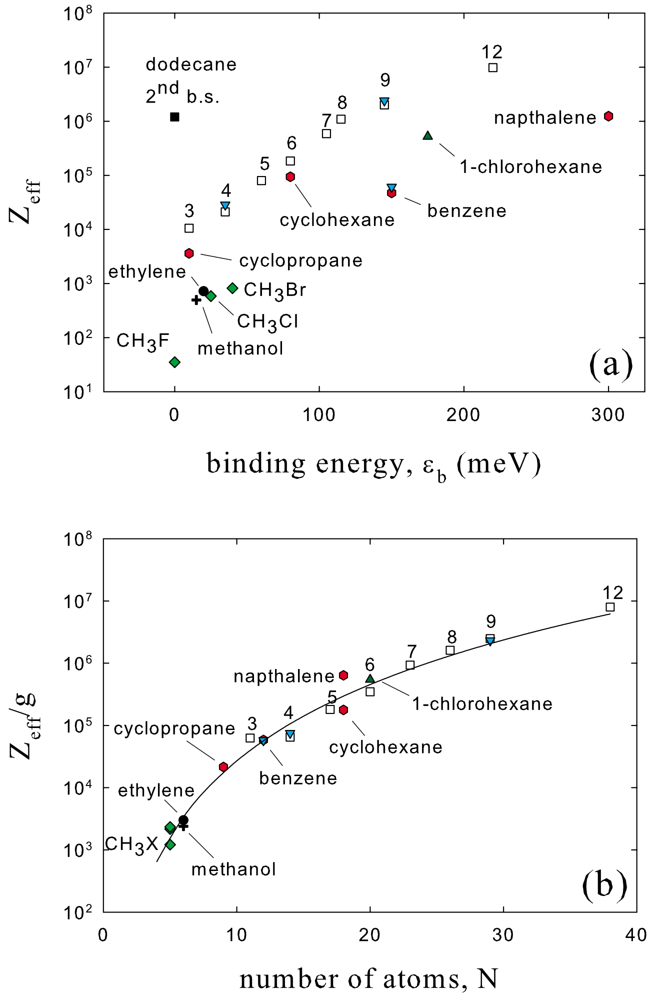

FIG. 5. (Color online) (a) Z_{eff} at the C-H stretch peak vs binding energy ϵ_b for alkanes, C_nH_{2n+2} (□); rings (red hexagons); halomethanes (green ◆); ethylene (●); methanol (+); 1-chlorohexane (dark green ▲); and deuterated species (cyan ▽). (b) Z_{eff} at the C-H stretch peak normalized by the factor $g=\sqrt{\epsilon_b/\epsilon}$ vs the number of atoms N in the molecule. For alkanes, the number of carbon atoms n is indicated. In (b), the solid line corresponds to the fit $Z_{\text{eff}}/g=2.3\times N^{4.1}$ described in the text. This plot demonstrates that Z_{eff} is insensitive to positron binding beyond the weak dependence g which is predicted by theory.

The fact that Z_{eff}/g depends so strongly on the number of atoms N (or essentially the number of vibrational degrees of freedom $3N-6$) has interesting implications. In the past, it has been suggested that the rapid growth of Z_{eff} is due to the fact that single-mode vibrational resonances act as "doorways" [14] whose energy may be transferred into a large reservoir of higher-order multimode vibrational excitations. This process, called IVR, results in an enhancement of Z_{eff} roughly proportional to the density of nearby states, which in turn, is expected to grow exponentially with the number of degrees of freedom. While experiments show that Z_{eff} does not grow as fast as the total vibrational mode density, as a simplified model would predict [14], the fact that Z_{eff} does grow rapidly with the number of vibrational degrees of freedom suggests that some form of IVR is occurring.

TABLE I. Physical parameters and annihilation data for various large molecules: number of atoms N; number of electrons Z; static dipole moment μ, in units of Debye [19]; dipole polarizability α [19,21]; ionization energy E_i [12,19]; annihilation rate for thermal positrons at room temperature $Z_{\rm eff}^{\rm th}$ [19]; experimentally determined positron binding energy ϵ_b annihilation rate at the C-H stretch VFR $Z_{\rm eff}^{\rm CH}$, and the normalized annihilation rate $Z_{\rm eff}^{\rm CH}/g$, using data from new and previous experiments [4–6,20]. Some values of α were calculated, using the method described in Ref. [21]. The binding energy is assigned the value "$\gtrsim 0$" if the molecule is VFR-active but ϵ_b was too small to measure.

Species	N	Z	μ [D]	α [Å^3]	E_i [eV]	ϵ_b [meV]	$Z_{\rm eff}^{\rm CH}$ [a]	$Z_{\rm eff}^{\rm th}$	$Z_{\rm eff}^{\rm CH}/g$
Alkanes									
methane	5	10	0	2.6	12.7			142	
ethane	8	18	0	4.44	11.52	$\gtrsim 0$	900	660	
propane	11	26	0.08	6.29	11.14	10	10500	3500	63000
butane	14	34	0	8.14	10.63	35	21000	11300	65000
pentane	17	42	0	9.98	10.35	60	80000	37800	180000
hexane	20	50	0	11.83	10.18	80	184000	120000	350000
heptane	23	58	0	13.68	9.9	105	590000	242000	930000
octane	26	66	0	15.52	10.03	115	1090000	585000	1610000
nonane[b]	29	74	0	17.37	10.02	145	2000000[b]	643000	2500000
dodecane	38	98	0	22.91	9.93	220	9800000	1780000	8000000
2nd BS	38	98	0	22.91	9.93	$\gtrsim 0$	1200000		
tetradecane	44	114		26.61		260	11x [c]		6.8x [b]
2nd BS	44	114		26.61		50	2.8x [c]		7.0x [c]
hexadecane	50	130	0	30.31	9.91	310	15y [c]	2230000	6.4y [c]
2nd BS	50	130	0	30.31	9.91	100	4.0y [c]		6.5y [c]
Alkane isomers									
isopentane	17	42	0.13	9.98	10.32	60	80000	50500	180000
Rings									
cyclopropane	9	24				10	3600		21500
cyclohexane	18	48	0	9.88	9.88	80	94000	20000	180000
benzene	12	42	0	10.4	9.25	150	47000	15000	58000
naphthalene	18	68	0	16.59	8.15	300	1240000	494000	640000
Haloalkanes									
1-fluoropropane	11	34		5.97		35	1520		4700
2,2-difluoropropane	11	42		5.88	11.42	25	900	8130	3300
1-fluorobutane	14	42		7.8		70	5600		11500
1-fluorohexane	20	58		11.46		80	60000 ± 30000	269000	110000 ± 60000
1-chlorohexane	20	66		13.59	10.3	175	520000		540000
1-fluorononane	29	82		16.98		145	930000		1150000
Deuterated									
d-benzene	12	68	0	10.4	9.25	150	61000	36900	57500
d-butane	14	34				35	28500		75000
d-nonane	29	74	0	17.37		145	2400000	641000	2300000
d-naphthalene	18	68				~300			

[a] As discussed in Sec. III, the true magnitudes of resonant $Z_{\rm eff}$ peaks will be larger than those measured here by a factor Δ/Γ, where Δ is the energy spread of the positron beam for the experiments reported here.

[b] $Z_{\rm eff}$ for nonane is from Fig. 7 as opposed to Ref. [5], which had a narrower positron energy distribution for this molecule.

[c] Absolute $Z_{\rm eff}$ could not be determined for these molecules, so their values are multiplied by the factors x and y.

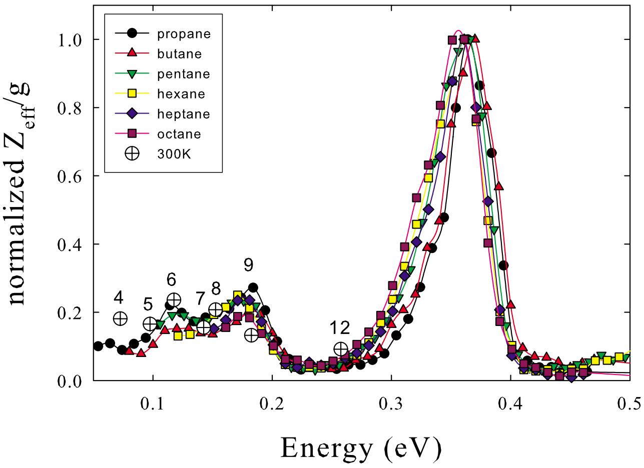

FIG. 6. (Color online) Normalized and energy-shifted Z_{eff}/g spectra for alkanes where $3 \leq n \leq 8$ carbons. For comparison, room temperature Z_{eff}/g data for alkanes are also shown at energies $\epsilon_b + \epsilon_T$, where $\epsilon_T = \frac{3}{2}kT = 37.5$ meV. Each room temperature datum is labeled by the number of carbons n in the measured alkane species. See text for details.

The lack of dependence of Z_{eff} on ϵ_b beyond that in the factor g is particularly interesting. A bound positron may not escape via deexcitation of a mode of energy ϵ_v, if $\epsilon_v < \epsilon_b$. Thus, increasing ϵ_b should block escape via these inelastic channels, resulting in an additional enhancement of Z_{eff} and a deviation from the "universal" curve in Fig. 5(b). However, there are few outliers to this curve. In this regard, the second bound state results for tetradecane or hexadecane should show a particularly large effect. Tetradecane has a factor ~6 difference in binding energy between its ground and first-excited states, but this produces virtually no change in Z_{eff}/g. Also, 1-chlorohexane has only a modest residual deviation from hexane after normalization. Thus, it appears that inelastic escape channels with more than a small amount of energy loss are inactive [22].

The key finding here is that the number of vibrational degrees of freedom in a molecule, not the positronic binding energy, is most important in determining the resonant annihilation rate. Furthermore, the dependence on binding energy seems to be almost completely described by the g factor. As a corollary, the fact that there are so few outliers to the universal scaling $Z_{eff}/g = 2.3 \times N^{\eta}$ provides indirect evidence that inelastic escape channels are relatively unimportant in determining the magnitude of the C-H stretch resonance in most hydrocarbons.

B. Relationship to thermal Z_{eff} at 300 K

In light of more recent, energy-resolved data for Z_{eff} [5,6] and their present interpretation (i.e., involving positron bound states, vibrational Feshbach resonances and IVR) [14], it is useful to examine previous measurements of large Z_{eff} for alkanes using Maxwellian distributions of positrons at 300 K [7–9,23]. Figure 6 shows a comparison of Z_{eff} spectra for alkanes with $3 \leq n \leq 8$ carbons. For each molecule, the magnitudes are normalized by $g = \sqrt{\epsilon_b/\epsilon}$, shifted upward in energy by ϵ_b, and then normalized to the C-H stretch peak magnitude. In this representation, it is clear that the spectra of alkanes change relatively little with molecular size. Each spectrum has a broad plateau in the range $50 < \epsilon + \epsilon_b < 170$ meV composed of C-C and C-H bend modes. The maximum of this plateau varies between 0.17 and 0.26 of the normalized C-H stretch peak magnitude. It is unclear why the spectral shape is so constant. In the context of the IVR model, one would expect the aforementioned ratio to decrease considerably with molecular size to reflect the growing disparity between the vibrational density of states at low and high energies.

As the size of an alkane increases, its Z_{eff} spectrum shifts to lower energies. Thus, a mode accessed at 50 meV in the butane spectrum will be accessed in hexane ($n=6$) at 5 meV by a thermal positron in a 300 K distribution. For this reason, one should expect the value of Z_{eff} measured at 300 K to be closely related to the corresponding value in the plateau. As shown in Fig. 6, the 300 K data align nicely with the energy resolved data when they are normalized by $g = \sqrt{\epsilon_b/\epsilon_T}$ (and the C-H stretch peak heights) and assigned a corrected energy of $\epsilon_b + \epsilon_T$, where $\epsilon_T = \frac{3}{2}kT = 37.5$ meV is the average thermal positron energy at 300 K. Note how alkanes with nine or more carbons, due to their larger binding, begin to sample the trough in the spectrum between the plateau and the C-H stretch peak. Thus, this analysis connects in a quantitative way the thermal data with the energy-resolved measurements, showing that thermal positrons at 300 K annihilate through IVR-enhanced vibrational Feshbach resonances.

C. Inelastic escape channels

There is a class of partially substituted alkanes for which Z_{eff}^{CH} is unusually small compared to alkanes of similar size. We refer to them as "suppressed-Z_{eff}" molecules. One example is 1-fluorononane, for which the Z_{eff} spectrum is shown in Fig. 7(a), where it is compared with that of nonane. The nonane spectrum used here was acquired under experimental conditions closer to those of other molecules presented in this paper. In contrast, the nonane spectrum in Ref. [5] used a slightly different technique which enhanced the energy resolution of C-H stretch peak while producing more scattering at low energy. The partially fluorinated molecules have C-H stretch peaks that are smaller by a factor of 2 or more than their nonsubstituted alkane counterparts [4–6]. To better understand this phenomenon, we examine the Z_{eff} spectra of additional fluoroalkanes. In particular, we look at 1-fluoropropane, 2,2-difluoropropane, 1-fluorobutane, and 1-fluorohexane.

A previous experiment on 1-fluorohexane was found to be in error, likely due to an air leak into the vacuum system. This experiment was repeated, and the results are shown in Fig. 7(b). At low energies, the Z_{eff} spectrum of 1-fluorononane is consistent with a previous measurement of thermal Z_{eff}, which indicated that Z_{eff} is 26 9000 for thermal positrons at 300 K [19,24]. For reasons that are presently unclear, there is significant variability in the measured magnitude of the C-H stretch peak for 1-fluorohexane—a problem that does not occur for the other partially fluorinated compounds.

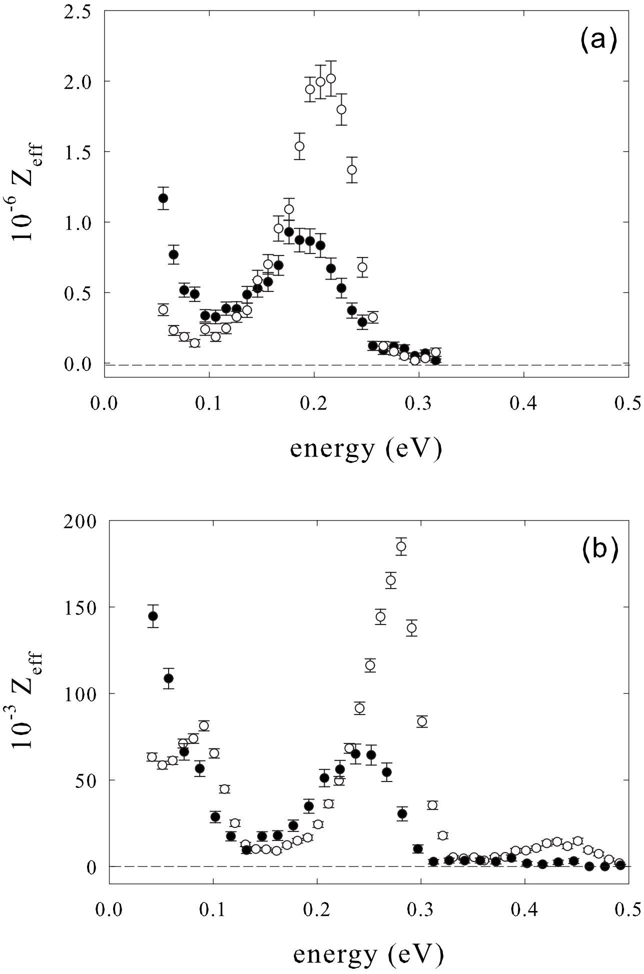

FIG. 7. (a) Z_{eff} spectra for (●) 1-fluorononane from Ref. [5] compared to that of (○) nonane and (b) (●) 1-fluorohexane compared to (○) hexane, also from Ref. [5]. There may be a ~50% error in the C-H stretch peak height of 1-fluorohexane. See the text for details.

As a result, we only trust the magnitude of the 1-fluorohexane data to within ~50%. That said, the C-H stretch peak in 1-fluorohexane is two to four times smaller than in hexane while the low energy peaks are larger than in hexane.

The Z_{eff} spectrum of 1-fluoropropane C_3H_7F was measured and compared to the previously measured spectra of propane (C_3H_8) and 2,2-difluoropropane ($C_3H_6F_2$) from Ref. [4]. As shown in Fig. 8, a number of interesting characteristics are apparent. Both 2,2-difluoropropane and 1-fluoropropane have much suppressed C-H stretch peaks that are smaller than that of propane by a factor of 5. Also, they both have low-energy peaks, with $Z_{\mathrm{eff}} \sim 4000$, that are the same magnitude as those in propane. This set of peaks drops in magnitude sharply near ~120 meV in both 1-fluoropropane and 2,2-difluoropropane (i.e., vertical dashed line in Fig. 8), while it persists until 200 meV in propane.

These Z_{eff} spectra indicate that the positron binding energies of propane, 1-fluoropropane, and 2,2-difluoropropane are 10, 35, and 25 meV, respectively. The slight extra reduction in the C-H stretch peak in 2,2-difluoropropane relative to 1-fluoropropane can be attributed to 2,2- difluoropropane's smaller binding energy and a slight reduction in number of C-H stretch modes. The molecules 2,2-difluoropropane and 1-fluoropropane appear to exhibit VFR very similar to those in small molecules such as ethanol [18], in that the low-energy features in the spectra dominate the C-H stretch peak.

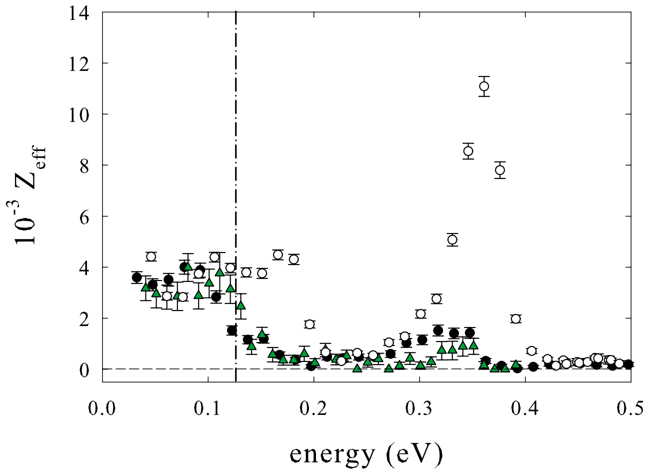

FIG. 8. (Color online) Z_{eff} spectra for (○) propane and (●) 1-fluoropropane (present work), and (green ▲) 2,2-difluoropropane from Ref [4]. The vertical dot-dash line (–·–) indicates the empirical position of an inelastic threshold (i.e., where the Z_{eff} magnitude is half of its low-energy value). See text for details.

The molecule 1-fluorobutane (C_4H_9F) exhibits behavior similar to the other partially fluorinated alkanes. As shown in Fig. 9, its C-H stretch peak is depressed by a factor of 5 relative to that of butane. It has a binding energy of 70 meV, which is larger than butane by 35 meV. The Z_{eff} suppression in 1-fluorobutane seems to end below a "threshold," indicated approximately by the vertical dot-dash line in Fig. 9. The low-energy Z_{eff} of 1-fluorobutane is ~18 000, which is ~2.5 times larger than that for butane. There is evidence of low-energy enhancements in other fluoroalkanes including 1-fluorononane [5,6], and based on thermal positron data, in 1-fluorohexane and 2,2-difluoropropane [6,19].

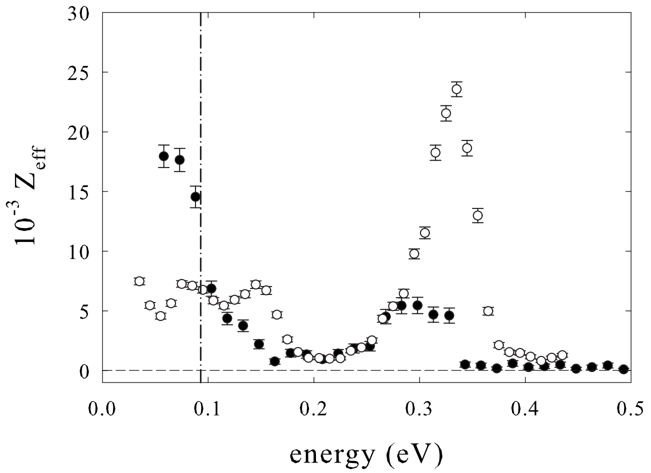

FIG. 9. Z_{eff} spectra for (○) butane and (●) 1-fluorobutane. The vertical dot-dash line (–·–) indicates the empirical position of the inelastic threshold. See text for details.

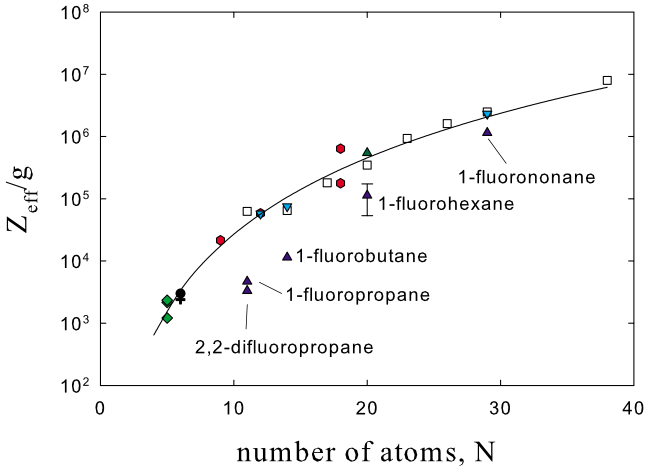

FIG. 10. (Color online) Normalized Z_{eff} at the C-H stretch peak vs number of atoms for a variety of species (similar to Fig. 5), including (blue ▲) suppressed-Z_{eff} molecules. The error bars on 1-fluorohexane indicate the unusually large uncertainty in this datum. The solid line shows the previously described $Z_{eff}/g=2.3\times N^{4.1}$ fit for unsuppressed molecules.

Figure 10 shows how these partially fluoronated hydrocarbons fit into the normalized Z_{eff} vs molecular size representation discussed in Sec. IV A. The 1-fluorohexane data point has been given large error bars to account for the experimental uncertainty. All of these molecules fall below the trendline for the other molecules. The suppression seems largest for the smaller molecules and gradually decreases to a factor of ~2.5 for 1-fluorononane. Extrapolating this trend, one could hypothesize that the suppression may well disappear completely in larger fluoroalkanes.

As suggested in Sec. IV A, this unusual reduction in Z_{eff} is likely the result of additional, inelastic escape channels. Gribakin has pointed out that the C-F stretch mode, in particular, may provide a strong inelastic escape channel [25]. It is worth noting that the vibrational inelastic excitation cross section for the asymmetric C-F stretch mode in CF_4 is as much as an order of magnitude larger than the vibrational excitation cross sections in other small molecules, due to its unusually strong dipole coupling [26].

The role of inelastic processes in VFR-mediated annihilation can best be understood by examining Eq. (1). According to the resonant annihilation theory [3], the integral contribution of a vibrational resonance ν to Z_{eff} is given by the expression

$$Z_{eff}^{res}\propto\Gamma_\nu^e\frac{\Gamma_\nu^a}{\Gamma_\nu^e+\Gamma_\nu^a+\Gamma^i}. \tag{3}$$

Here Γ_ν^e describes the rate of positron capture, while $\Gamma_\nu^a/\Gamma_\nu^e+\Gamma_\nu^a+\Gamma^i$ describes the probability of positron annihilation in the resonant state, which competes with both elastic (Γ_ν^e) and inelastic (Γ^i) reemission. If one ignores the latter term and assumes that Γ_ν^e is the dominant factor, the rate factors cancel and $Z_{eff}\propto\Gamma_\nu^a/k\propto g$, as before. However, if $\Gamma_\nu^i>\Gamma_\nu^e$, there will be steplike reductions in Z_{eff} above the threshold for each inelastic channel [3]. This is consistent with the behavior observed in the fluoroalkane experiments (e.g., dot-dashed lines in Figs. 8 and 9).

There are two types of inelastic processes that could be involved: resonant excitation and deexcitation. The former leaves the molecule with one more quantum of energy ω_i similar in this sense to nonresonant vibrational excitation [26]. The latter leaves the free positron with energy $\omega_i-\epsilon_b$ and the remaining energy with the molecule. Defining ω_ν as the energy of the initial excitation (e.g., the C-H stretch mode) and M is the molecule, the resonant excitation and deexcitation processes are, respectively,

$$e^+(\omega_\nu-\epsilon_b)+M(0)\to e^+(\omega_\nu-\omega_i-\epsilon_b)+M(\omega_i) \tag{4}$$

and

$$e^+(\omega_\nu-\epsilon_b)+M(0)\to e^+(\omega_i-\epsilon_b)+M(\omega_\nu-\omega_i). \tag{5}$$

Note that both $\omega_\nu-\omega_i$ and ω_i must correspond to energies of single or multimode vibrational excitations.

Both processes involve bound-continuum transitions [15] rather than continuum-continuum transitions [26]. In the Born-dipole approximation, the inelastic widths for these processes are proportional to the square of the transition dipole moments [15]. As a result, both processes are dipole-forbidden because they require a two-quantum change. However, if there is a strong coupling $\gamma_{\nu x}$ between the initial excitation ν and an intermediate multimode excitation x that contains the mode of interest, a single quantum deexcitation is possible, resulting in ejection of the positron.

The transition dipole moment for this resonant deexcitation process is $\gamma_{\nu x}d_i$, where d_i is approximately equal to the ground-state transition dipole for mode i [27]. Thus, if i is the C-F stretch mode, the capture width is proportional to the strong, dipole-allowed C-F stretch transition. This is the same strong dipole coupling that results in the large, vibrationally inelastic cross sections for e^+-CF_4 collisions [26]. Note that the inelastic width is modulated by $\gamma_{\nu x}$, which depends on the density of multimode states containing the C-F stretch vibration. This density generally decreases with energy and becomes zero when $\omega_\nu<\omega_i$.

Judging from the location at which the Z_{eff} drops by a factor of 2 in the smaller fluoroalkanes (i.e., dot-dashed lines in Figs. 8 and 9), the energy of the deexcitation escape mode is ~155 meV. Suppression can only occur if the positron can escape, i.e., $\epsilon_b\leq 155$ meV. The binding energies of both 1-fluorohexane and 1-fluorononane are consistent with this condition (the latter has a binding of ~145 meV). Thus it is likely that this inelastic channel is due to the C-F stretch mode, although it occurs at a slightly higher energy than expected [28].

This explanation resolves the long standing question as to why fluoroalkanes behave differently than alkanes [5,6]. It suggests that the fluoroalkanes have a strong, C-F stretch-mediated resonant inelastic channels that cause suppression of Z_{eff} above a certain energy. It also provides evidence for resonant coupling between the C-H stretch mode and an "intermediate" multimode vibration, which is required for this inelastic channel. In a sense, the presence of this state provides indirect evidence that mode-mixing processes, such as IVR, are possible. The molecule 1-chlorohexane exhibits no such suppression even though the C-Cl stretch mode quite likely has strong dipole coupling to the positron. This is to be expected, since this inelastic escape channel is forbidden due to the fact that the C-Cl mode energy is smaller than the binding energy in this molecule, and so the inelastic escape process is energetically forbidden.

D. Dependence of Z_{eff} on molecular temperature

In principle, thermally excited modes can stimulate positron detachment, contributing to the overall inelastic width and suppressing Z_{eff}. In the simplest picture, the probability that a given degree of freedom has sufficient energy to unbind the positron decreases exponentially with binding energy at a rate proportional to the Boltzmann factor $\exp(-\epsilon_b/k_B T)$, where k_B is the Boltzmann constant and T is the temperature. As T decreases, so does the probability of thermal detachment, which should result in an increase in Z_{eff} determined by the binding energy and the mode density.

Recently, a specially designed cold cell was used to measure Z_{eff} as a function of temperature for two alkane molecules, pentane (C_5H_{12}) and heptane (C_7H_{16}) [13]. Pentane was measured at 153 K and 15.5 μTorr and heptane at 195 K and 1.34 μTorr. The positions of the Z_{eff} peaks are unaltered when the temperature is changed, indicating that there is little or no change in the binding energies. For both molecules, there was relatively little change in the magnitude or shape of Z_{eff} in response to the significant change in temperature. Most of the change in Z_{eff} that did occur was observed at lower positron impact energies. Specifically, at low temperature and smaller values of positron energy, Z_{eff} increased by ~30% in pentane and ~50% in heptane [13].

This lack of a strong temperature dependence of Z_{eff} eliminates any possible Boltzmann-type scaling of Z_{eff} with binding. If that scaling were correct, the C-H stretch peak in pentane should have grown by a factor of 10 as the temperature was lowered by the amount indicated. In general, inelastic positron detachment by thermal modes appears to be a relatively weak process in these molecules.

The temperature-independence of the binding energy also tends to rule out one model of positron binding energy. In particular, it was suggested that a change in the bond geometry might be required for a positron to bind to a molecule (and hence also required for VFR-mediated annihilation) [29,30]. It was postulated that binding could occur only if the molecule were in a highly excited vibrational state. One way to control the level of vibrational excitation is to change the temperature (i.e., "hot" molecules would be expected to have deeper binding than "cold" molecules). By extension, hot molecules would also be more likely to have VFR annihilation peaks (or to have larger peaks). The cold-cell data show no evidence of this effect. The binding energy is constant over approximately a factor of 2 change in molecular temperature.

E. Other effects

In addition to the anomalies discussed in Sec. IV C, there are other, moderate-sized departures from the universal scaling $Z_{\mathrm{eff}}/g \propto N^{4.1}$. According to the doorway-state IVR model, Z_{eff} is roughly proportional to the density of "dark" vibrational states at the resonance energy [14]. In this context, the empirical scaling law describes how this density of "dark" states grows with the number of atoms or the vibrational degrees of freedom. Both 1-chlorohexane and the large 1-fluoroalkanes (below the inelastic threshold) have slightly enhanced Z_{eff}/g compared to similarly sized alkanes. This enhancement likely reflects higher-order changes in their dark state densities. In both cases, a few high energy C-H modes are converted into lower energy C-X modes where X is a halogen, resulting in a higher density of vibrational states at a given energy.

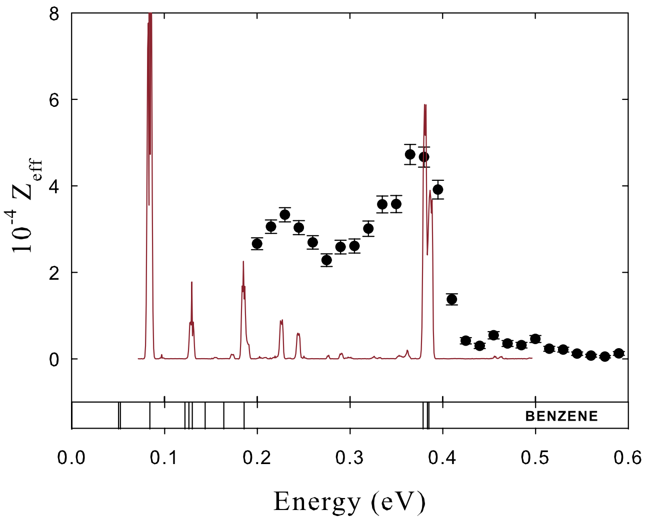

FIG. 11. (Color online) Energy-resolved Z_{eff} (●) and infrared absorption spectrum (—) for benzene. The Z_{eff} spectrum has been shifted upward by the binding energy $\epsilon_b = 150$ for direct comparison, and the normalization of the IR absorption [12] is arbitrary. The lower panel indicates the positions of the vibrational modes in benzene from Ref. [12].

The previous section introduced the possibility of intermediate states that stand between the capture state (e.g., the C-H stretch vibration) and the final bath of "dark" states. In the fluoroalkanes, such intermediate states are necessary for an effective inelastic escape channel. This suggests that post-capture dynamics may be represented more accurately by a tiered IVR model such as that described in Ref. [31], rather than the simpler two-step IVR discussed thus far. This results in a number of higher-order effects that might be indirectly observed by comparing spectra from partially deuterated species (see Ref. [32]). For further discussion of this topic, see Ref. [18].

Most resonances in large molecules occur near vibrational fundamentals. However, there are some exceptions. As shown in Fig. 11, there is a sizable feature in benzene that, after correcting for binding, corresponds to a vibrational mode at ~235 meV. While there are no fundamental modes at this energy, there is a pair of dipole-active combination modes at 227 and 244 meV. These vibrations appear to produce surprisingly strong peaks in the infrared spectrum, which is shown in Fig. 11. The observed feature in Z_{eff} appears to be due to strong, multimode VFR. This is unusual since multimode VFR-mediated annihilation is typically not

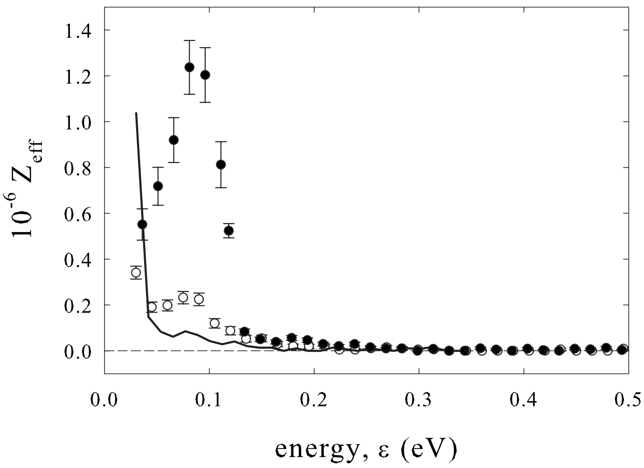

FIG. 12. Energy-resolved Z_{eff} for (●) naphthalene and (○) deuterated naphthalene. Also shown is (—) the naphthalene spectrum with the energy scaled by the ratio of C-H and C-D stretch mode energies (after correcting for binding), and the magnitude is scaled by the ratio of the *g* factors. Note that only the tail of the C-H stretch peak can be seen after this scaling.

observed in large molecules [4–6]. The only other evidence of combination or overtone VFR is in small and intermediate-sized molecules, such as methanol, where there is little or no IVR [11]. It is not clear why benzene is special in this regard.

F. Very large hydrocarbons and second bound states

As discussed in Sec. IV A and Refs. [6,15,20], hydrocarbons with ten or more carbons have some of the largest binding energies and peak Z_{eff} measured to date. Among these larger hydrocarbons is naphthalene ($C_{10}H_8$), a two-ring aromatic molecule and the smallest of a class of molecules called polycyclic aromatic hydrocarbons (PAHs). The energy-resolved Z_{eff} spectrum for naphthalene is shown in Fig. 12. There is a large uncertainty in the overall magnitude of the spectrum because of the uncertainty in absolute pressure, as described in Sec. III. That said, the magnitude of the single peak at 80 meV is 1.2×10^6, similar in magnitude to the C-H stretch peak of octane. It is natural to associate this peak with the C-H stretch mode, since there are no strong peaks at higher energy. This implies that naphthalene has a huge binding energy of 300 meV—larger than that of tetradecane (i.e., the 14 carbon alkane) and twice that of benzene. Possible reasons for this large value of binding energy are discussed in Sec. IV G below. Note that unlike tetradecane, there is no evidence of a second bound state.

The Z_{eff} spectrum of deuterated naphthalene (*d*-naphthalene) is also shown in Fig. 12. Here we assume similar ion gauge calibration factors for the protonated and deuterated molecules, so that absolute comparisons can be made. The black line in Fig. 12 shows the predicted Z_{eff} spectrum for *d*-naphthalene, assuming the observed peak in naphthalene is due to the C-H stretch VFR. As predicted, there is a significant upswing in the Z_{eff} of *d*-naphthalene at low energies, which is absent in naphthalene and likely due to the C-D stretch mode. There is also another peak around 80 meV with a modest Z_{eff} of 2.5×10^5, the origin of which is not presently understood [33]. See Ref. [18] for further discussion.

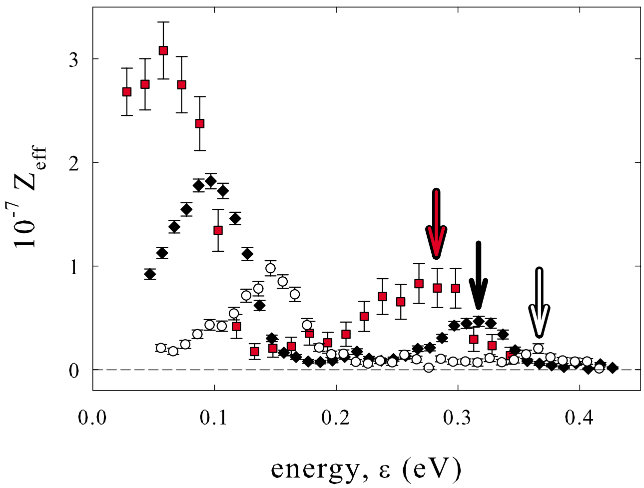

FIG. 13. (Color online) Z_{eff} spectra for (○) dodecane, (◇) tetradecane, and (□) hexadecane. The vertical arrows indicate the positions of the C-H stretch mode VFR peaks for the second bound state (i.e., positronically excited state) in each molecule. The spectra for tetradecane and hexadecane have been arbitrarily normalized (see text for details). The large peaks at lower energy are the C-H stretch mode VFR for the first bound states (the positronic ground states).

Measurements for dodecane ($C_{12}H_{26}$) and tetradecane ($C_{14}H_{30}$) [6] are shown in Fig. 13, and a recent measurement for hexadecane ($C_{16}H_{34}$) is included from Ref. [20]. Because of the difficulties in measuring the pressures for these compounds, similar to those discussed above for naphthalene, the absolute magnitudes of the tetradecane and hexadecane spectra are uncertain. In this case, there are no comparable ionization gauge data available, and so these Z_{eff} spectra are scaled arbitrarily.

The Z_{eff} for dodecane is huge, approaching 10^7. Note also the nearly linear downward shift of the dominant C-H stretch peak with increasing molecular size. This continues the trend of binding energies increasing with molecular size that was observed in smaller alkanes [4,5]. There is now a second, weaker peak just slightly below the C-H stretch mode. This peak shifts downward and increases in magnitude as the size of the alkane increases. Measurements of Z_{eff} as a function of pressure eliminate the possibility that this peak is a spurious three-body effect. That this peak is due to multimode VFR is theoretically possible but unlikely. It appears that this peak is the C-H stretch VFR associated with a second, positronically excited bound state [6]. The positron-molecule potential has now become deep enough to support a second bound state. Such excitation of higher positron bound states have recently been predicted in calcium atoms using configuration-interaction methods [34]. They are also predicted in molecules in the framework of the less rigorous, zero-range potential (ZRP) model for alkanes [15], which is discussed in the next section.

Data for the first and second bound states are shown in Table II. As can be seen in this table, the binding energies of

TABLE II. Binding energy and Z_{eff} data for molecules with second bound states. The values $\epsilon_b^{(1)}$ and $\epsilon_b^{(2)}$ refer to the energies of the first and second bound states; $Z_{\mathrm{eff}}^{(1)}/Z_{\mathrm{eff}}^{(2)}$ is the ratio of first and second bound state C-H stretch mode peak heights; and $g^{(1)}/g^{(2)}$ is the ratio of the g scaling factors. Naphthalene is included to demonstrate that chemical structure appears to play an important role in determining which molecules have positronically excited states.

Species	$\epsilon_b^{(1)}$ [meV]	$\epsilon_b^{(2)}$ [meV]	$Z_{\mathrm{eff}}^{(1)}/Z_{\mathrm{eff}}^{(2)}$	$g^{(1)}/g^{(2)}$
dodecane ($C_{12}H_{26}$)	220	≥ 0	8.17	≥ 0
tetradecane ($C_{14}H_{30}$)	260	50	3.94	3.79
hexadecane ($C_{16}H_{34}$)	310	100	3.83	3.69
naphthalene ($C_{10}H_8$)	300			

both the first and second bound states grow by 20–25 meV per carbon, which continues the trend observed in the smaller alkanes [4]. Furthermore, the ratio of the first and second bound state peaks obeys the scaling $Z_{\mathrm{eff}}^{(1)}/Z_{\mathrm{eff}}^{(2)} = g^{(1)}/g^{(2)}$ for both hexadecane and tetradecane. In order for this equality to work for dodecane, the binding energy of the second bound state would be ~8 meV, which is within our experimental error. Thus, the g factor robustly describes the magnitudes of both the first and second bound state VFR, even for binding energies of 300 meV. Note the conspicuous absence of a second bound state in naphthalene, in spite of the large binding energy of the first bound state. This contrast in behavior from that in the alkanes is not presently understood.

G. Positron-molecule binding energies

In a recent paper [15], Gribakin and Lee calculated positron binding energies for alkanes using a ZRP model. In this approximation, the positron interaction with each monomer is represented by a zero-range potential with inverse scattering length κ_i. The positron binding energy ϵ_b can then be determined from $\kappa = \sqrt{2\epsilon_b}$, where κ is the overall inverse scattering length in the limit of vanishing κ. The results of this calculation are shown in Fig. 14. Initially, κ_i was chosen to reproduce the experimental binding energy of propane (i.e., the smallest alkane with a well-resolved positron binding energy) [15]. Later κ_i was optimized to dodecane [35].

Qualitatively, the theory reproduces key features seen in experiment. The binding energy increases with the number of carbons and a second bound state appears not far from the experimentally observed onset at 12 carbons. The more recent, dodecane-based model provides the best fit to the data. However, both ZRP models produce binding energies that are moderately nonlinear with the number of carbons in contrast with experiment. As a result, the propane-based model overestimates binding energies by a factor of 2 in large molecules while the dodecane-based model incorrectly predicts no binding for molecules with less than four carbons. Clearly a more sophisticated model is required to correct these issues, perhaps taking into account additional factors such as molecular polarizability.

The ZRP model depends on knowing the strengths of the positron-molecule coupling to elements of the molecule (i.e., a set of scattering lengths κ_i) [15]. This makes it difficult to predict positron binding energies for other molecular species. In order to gain a better understanding of what determines the positron binding energy, in Fig. 15, we show binding energy vs molecular polarizability α for a variety of species. At large distances, the polarizability produces an attractive potential $-\alpha e^2/2r^4$ in response to the positron charge. Ignoring short-range effects such as nuclear repulsion and virtual Ps formation, it is expected that binding energy should increase with molecular polarizability.

As expected, binding energies generally increase with polarizability. This is most clear for the alkanes and their second bound states. Data for other hydrocarbons studied to date all lie slightly above the alkane curve. The most signifi-

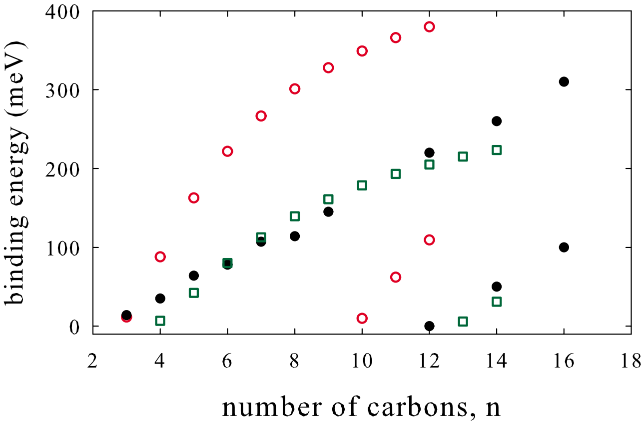

FIG. 14. (Color online) Experimental values of binding energies (●) for the first and second bound states in alkanes (C_nH_{2n+2}) [5,6,20] are shown as a function of the number of carbons n and compared to predictions of the ZRP model. Plotted here is the original model for a chain of ZRP monomers with κ_i optimized to propane (○) [15] as well as a more recent fit to dodecane (□) [35].

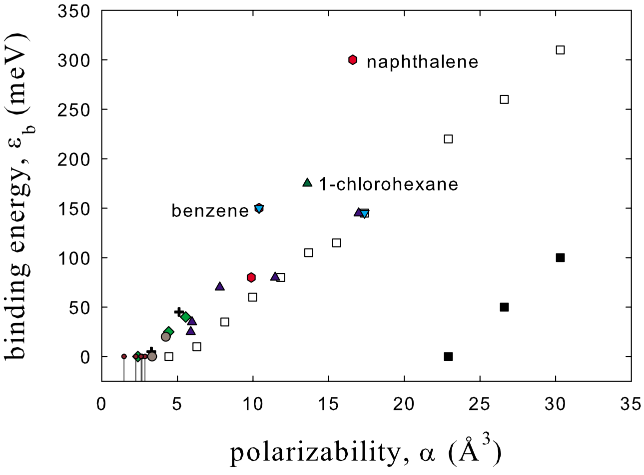

FIG. 15. (Color online) Binding energy vs polarizability for alkanes (□); alkane second bound states (black ■); rings (red hexagons); halomethanes (green ◇); acetylene and ethylene (gray ●); alcohols (+), 1-chlorohexane (dark green ▲); fluoroalkanes (blue ▲); and deuterated species (cyan ▽). VFR-weak or inactive species (small red ●) have a drop line to indicate possible "negative" binding energies (i.e., virtual states).

cant outliers are benzene, naphthalene, and 1-chlorohexane—molecules that have unusually large binding energies for their sizes. Benzene and naphthalene have significantly lower ionization potentials than comparably sized molecules, which may result in reduced repulsion at short distances. While the ionization potential of 1-chlorohexane is not remarkable, perhaps its sizable static dipole moment results in a larger binding energy.

By itself, the ionization energy E_i is a much weaker predictor of positron binding energies in large molecules. Only especially high or low ionization energies seem to affect binding. Simple alkanes with six or greater carbons all have ionization energies ~ 10 eV. Deeply bound species such as benzene and naphthalene have unusually small ionization energies (9.25 and 8.12 eV, respectively). Perfluoroalkanes have unusually high ionization energies, possibly indicating that they do not form bound states.

As discussed in Ref. [18], there is a somewhat improved correlation between the larger binding energies and the combination of parameters α^2/N, where N is the number of atoms. In a weak binding model, this would imply that $\kappa \propto \alpha/\sqrt{N}$, giving slightly reduced positron attraction for molecules with greater volume. In general, these results show some tantalizing patterns. As the data set grows, it is probably worth pursuing an extension to the ZRP model or an empirical addition law, similar to those used for predicting polarizabilities in molecules (see Ref. [21]). Such approximation schemes have the potential to reduce greatly the labor required to estimate positron binding energies.

V. CONCLUDING REMARKS

It is shown here that the magnitudes of the resonant Z_{eff} peaks observed in positron-molecule interactions depend only weakly on incident positron energy and positron-molecule binding energies via a scale factor $g = \sqrt{\epsilon_b/\epsilon}$. After this dependence is removed, most molecules follow a universal scaling $Z_{\text{eff}}/g \propto N^{4.1}$, where N is the number of atoms. A successful, quantitative connection is made between the Z_{eff} values measured with thermal positrons at 300 K and the energy-resolved measurements of vibrational Feshbach resonances observed at higher positron energies. Physically, we interpret the dependence on N as a dependence on the number of vibrational degrees of freedom of the molecule. We argue that this binding-energy independent scaling implies, in turn, that the enhanced Z_{eff} are likely caused by IVR with inelastic escape channels that are either weak or inactive. Similarly, the role of thermally excited inelastic escape channels appears to be limited, based upon the observed weak dependence of resonant Z_{eff} on target gas temperature in alkanes. While it is compelling that the observed rapid increase of Z_{eff} with increasing N is due to coupling to dark states, there is, as yet, no quantitative understanding of this effect. Understanding the physics underlying this universal scaling is a key problem for future research.

The only major exception to this scaling is the case of the partially fluorinated alkanes. In these molecules, Z_{eff} is suppressed above a threshold energy, providing evidence for a strong, deexcitation escape channel via the C-F stretch mode. This implicitly relies on coupling to intermediate, multimode excitations following capture.

Additional effects are observed in large molecules. In benzene, there is evidence of strong multimode VFR, which is absent in other large molecules studied to date. In molecules such as 1-chlorohexane, there is an enhancement in Z_{eff} beyond that given by the universal scaling. Furthermore, the scaling with N does not directly address the magnitudes of the VFR-enhanced annihilation peaks other than the C-H stretch resonance. There is at present no theory that explains the relative magnitudes of the VFR at lower energies (including those inferred from thermal positron data) and the fact that, in alkanes, these resonances are nearly constant in magnitude relative to the C-H stretch mode VFR. These behaviors can possibly be described in terms of changes in the number of dark states and intermediate states in a tiered IVR model [18].

With regard to positron-molecule binding energies, benzene, naphthalene, and 1-chlorohexane all have unusually large binding for their sizes, relative to the alkanes. In addition, large alkanes exhibit additional positronically excited bound states. These positron binding energies are, at present, difficult to calculate in any molecule, especially larger molecules. Positron binding appears to be roughly correlated with increases in such parameters as the dipole polarizability and the number of atoms, and weakly anticorrelated with increases in the molecular ionization energy. It is hoped that the experimental measurements of binding energies presented here will stimulate further theoretical efforts to calculate them.

ACKNOWLEDGMENTS

We thank Gleb Gribakin, Chris Lee, and James Danielson for helpful conversations, and Gene Jerzewski for technical assistance. This work was supported by National Science Foundation Grant No. PHY 02-44653.

---

[1] M. Charlton and J. Humberston, *Positron Physics* (Cambridge University Press, New York, 2001).

[2] C. M. Surko, G. F. Gribakin, and S. J. Buckman, J. Phys. B **38**, R57 (2005).

[3] G. F. Gribakin, Phys. Rev. A **61**, 022720 (2000).

[4] S. J. Gilbert, L. D. Barnes, J. P. Sullivan, and C. M. Surko, Phys. Rev. Lett. **88**, 043201 (2002).

[5] L. D. Barnes, S. J. Gilbert, and C. M. Surko, Phys. Rev. A **67**, 032706 (2003).

[6] L. D. Barnes, J. A. Young, and C. M. Surko, Phys. Rev. A **74**, 012706 (2006).

[7] D. A. L. Paul and L. Saint-Pierre, Phys. Rev. Lett. **11**, 493

(1963).

[8] G. R. Heyland, M. Charlton, T. C. Griffith, and G. L. Wright, Can. J. Phys. **60**, 503 (1982).

[9] C. M. Surko, A. Passner, M. Leventhal, and F. J. Wysocki, Phys. Rev. Lett. **61**, 1831 (1988).

[10] G. F. Gribakin and C. M. R. Lee, Phys. Rev. Lett. **97**, 193201 (2006).

[11] J. A. Young, G. F. Gribakin, C. M. R. Lee, and C. M. Surko (unpublished).

[12] NIST Chemistry WebBook, 2005, URL http://webbook.nist.gov/chemistry/

[13] J. A. Young and C. M. Surko, Nucl. Instrum. Methods Phys. Res. B **266**, 478 (2008).

[14] G. F. Gribakin and P. M. W. Gill, Nucl. Instrum. Methods Phys. Res. B **221**, 30 (2004).

[15] G. F. Gribakin and C. M. R. Lee, Nucl. Instrum. Methods Phys. Res. B **247**, 31 (2006).

[16] G. Gribakin, in *New Directions in Antimatter Physics and Chemistry*, edited by C. M. Surko and F. A. Gianturco (Kluwer Academic Publishers, Dordrecht, 2001), pp. 413–435.

[17] L. D. Barnes, J. P. Marler, J. P. Sullivan, and C. M. Surko, Phys. Scr. **110**, 280 (2004).

[18] J. A. Young, Ph.D. thesis, University of California, San Diego, 2007.

[19] K. Iwata, Ph.D. thesis, University of California, San Diego, 1997.

[20] J. A. Young and C. M. Surko, Phys. Rev. Lett. **99**, 133201 (2007).

[21] K. J. Miller and J. A. Savchick, J. Am. Chem. Soc. **101**, 7206 (1979).

[22] In Sec. IV C, we discuss annihilation in partially fluorinated alkanes, which provide a striking exception to this behavior.

[23] K. Iwata, R. G. Greaves, T. J. Murphy, M. D. Tinkle, and C. M. Surko, Phys. Rev. A **51**, 473 (1995).

[24] Based on the vibrational mode spectrum of 1-fluorohexane, there is probably a VFR at ~25 meV.

[25] G. F. Gribakin (private communication).

[26] J. P. Marler, G. F. Gribakin, and C. M. Surko, Nucl. Instrum. Methods Phys. Res. B **247**, 87 (2006).

[27] The dipole moment d_i is not a true ground-state transition because it leaves the molecule in a partially excited state.

[28] According to Ref. [12], the C-F stretch mode energy in CH_3F is 120 meV.

[29] T. Nishimura and F. A. Gianturco, Europhys. Lett. **68**, 377 (2004).

[30] T. Nishimura and F. A. Gianturco, Phys. Rev. A **72**, 022706 (2005).

[31] V. May and O. Kühn, *Charge and Energy Transfer Dynamics in Molecular Systems* (Wiley VCH, New York, 2000).

[32] Y. Yamada, N. Mikami, and T. Ebata, J. Chem. Phys. **121**, 11530 (2004).

[33] Slight contamination by protonated naphthalene, in spite of very thorough baking, cannot be completely ruled out.

[34] M. W. J. Bromley and J. Mitroy, Phys. Rev. A **75**, 042506 (2007).

[35] C. M. R. Lee, Ph.D. thesis, Queen's University, Belfast, 2006.